Geophysical Research Letters

RESEARCH LETTER
10.1029/2025GL118406

In Situ Observations Reveal That the South Asian Summer Monsoon Weakens Aerosol Cloud Activation Over the Southern Tibetan Plateau

Zhao Ji[1], Yuan Wang[1], Jiming Li[1], Ping Zhang[1], Fang Fang[1], Qiudi Xu[1], Ruling Lv[1], Jinsen Shi[1], and Jianping Huang[1]

[1]Collaborative Innovation Center for Western Ecological Safety, College of Atmospheric Sciences, Lanzhou University, Lanzhou, China

Key Points:

- Aerosols over Southern Tibetan Plateau (TP) exhibit weak cloud activation capacity during the South Asian Summer Monsoon
- Aerosol concentration and activation capacity over the Southern TP are negatively correlated with the monsoon intensity
- Orographic uplift of monsoonal air over the southern plateau enhances cloud formation and wet scavenging, suggesting a plausible mechanism

Supporting Information:

Supporting Information may be found in the online version of this article.

Correspondence to:

Y. Wang,
wang_yuan@lzu.edu.cn

Citation:

Ji, Z., Wang, Y., Li, J., Zhang, P., Fang, F., Xu, Q., et al. (2025). In situ observations reveal that the South Asian summer monsoon weakens aerosol cloud activation over the Southern Tibetan Plateau. *Geophysical Research Letters*, *52*, e2025GL118406. https://doi.org/10.1029/2025GL118406

Received 23 JUL 2025
Accepted 16 DEC 2025

Author Contributions:

Conceptualization: Yuan Wang
Data curation: Jiming Li
Formal analysis: Zhao Ji, Yuan Wang, Jiming Li, Ping Zhang, Fang Fang, Qiudi Xu, Ruling Lv
Funding acquisition: Yuan Wang, Jiming Li, Jinsen Shi, Jianping Huang
Investigation: Yuan Wang, Ping Zhang, Fang Fang, Jinsen Shi
Methodology: Zhao Ji, Yuan Wang
Project administration: Yuan Wang, Jiming Li, Jianping Huang
Software: Qiudi Xu
Supervision: Yuan Wang
Visualization: Zhao Ji, Ping Zhang

Abstract The South Asian Summer Monsoon (SASM) strongly influences aerosol and moisture transport over the Tibetan Plateau (TP), shaping its environment and climate. However, its impact on aerosol activation remains unclear due to limited observations. Here, in situ measurements at Mount Qomolangma Station during the 2024 SASM reveal weak aerosol activation capacity over the southern TP, with hygroscopicity parameter values mostly below 0.1 and daily-mean cloud condensation nuclei (CCN) concentrations at 0.2% supersaturation ranging from 5 to 282 cm^{-3}. Notably, CCN concentration, activation fraction, and hygroscopicity all exhibit significant negative correlations with SASM intensity, suggesting that stronger monsoonal transport reduces aerosol activation as clouds. This weakening is attributed to orographic lifting of monsoon air masses, which enhances cloud formation, precipitation, and wet scavenging, depleting CCN during upslope transport before the airmass reaches Qomolangma. These findings have important implications for understanding cloud formation and aerosol–cloud interactions over this climatically sensitive region.

Plain Language Summary Cloud condensation nuclei (CCN), often referred to as the "seeds" of clouds, play a crucial role in determining cloud properties such as thickness and lifetime. The South Asian Summer Monsoon transports aerosols, including CCN, from the Indian subcontinent to the Tibetan Plateau (TP). It might be expected that stronger monsoon activity would deliver more CCN to the Plateau. However, in situ observations at Mount Qomolangma Station reveal the opposite: as monsoon intensity increases, fewer aerosols and CCN reach the Plateau, at least in the near-surface layer. This occurs because moist monsoonal air, when lifted by the southern slopes of the TP to altitudes exceeding 4,000 m, promotes cloud and precipitation formation, which in turn removes not only aerosol particles in general but preferentially those with higher activation potential (i.e., larger size and greater hygroscopicity), thereby reducing the CCN activity of the remaining aerosol population over the southern TP. This has important implications for understanding cloud formation and aerosol–cloud interactions in this climatically sensitive region.

1. Introduction

Cloud condensation nuclei (CCN) activation constitutes the initial and critical step in warm cloud formation. Together with ambient water vapor supersaturation, CCN activation governs the cloud droplet number concentration, which in turn influences cloud microphysical properties, precipitation formation and climate (Charlson et al., 1992; Pöhlker et al., 2023; Prabhakaran et al., 2020; Stevens & Feingold, 2009; Stier et al., 2024; C. Zhao et al., 2024). As the focus of aerosol–cloud interaction research, CCN activation has been extensively observed and studied across diverse environments, including urban and suburban (e.g., Bhattu & Tripathi, 2014; Deng et al., 2011; Patidar et al., 2012; Rejano et al., 2021; Salma et al., 2021; Yuan & Zhao, 2023), rural (e.g., Kuang et al., 2024; Singla et al., 2017; Tao et al., 2021; Y. Wang et al., 2022), tropical rainforest (e.g., Gunthe et al., 2009; Irwin et al., 2011; Pöhlker et al., 2016), coastal (e.g., Bougiatioti et al., 2016; Gong et al., 2019; Jayachandran et al., 2018), and high-altitude remote regions (e.g., Jayachandran et al., 2018; Rejano et al., 2024; Shen et al., 2025; J. Z. Xu et al., 2024).

Known as the Third Pole of the world and the Water Tower of Asia, the Tibetan Plateau (TP) plays a critical role in regulating the regional water cycle and climate through its cloud systems (Kang et al., 2022; Liu et al., 2020; Y. Ma et al., 2017). However, limited in situ observations have hindered a clear understanding of cloud formation processes in this region. Y. Wang et al. (2024) conducted in situ GACPE-STP campaign and found that from

Writing – original draft: Zhao Ji
Writing – review & editing: Yuan Wang

August to October 2023, the CCN activation capacity at Yadong Station (27.42°N, 88.90°E; 3136 m a.s.l.) on the southern TP slope was notably weak. Specifically, mean CCN concentrations and activation fractions at supersaturations ranging from 0.07% to 0.7% varied from 24 to 483 cm^{-3} and 2%–48%, respectively, and aerosol hygroscopicity values derived from multiple measurement schemes (Methods Section in Y. Wang et al., 2024) were consistently below 0.1, which is well below the continental reference value of 0.3 ± 0.1 suggested by Andreae and Rosenfeld (2008). Y. Wang et al. (2024) primarily attributed the weak activation to distinctive local emissions over the Southern TP. However, the potential influence of the South Asian Summer Monsoon (SASM) on aerosol activation capacity over the TP remains unexplored.

The SASM is a major pathway for the transport of moisture, aerosols, and energy from the Indian subcontinent to the TP (Fadnavis et al., 2017; Guo et al., 2025; Kang et al., 2022). From May to September, the SASM carries abundant water vapor from the Indian Ocean and the Bay of Bengal, driving widespread precipitation over South Asia (B. Wang et al., 2009; Webster & Yang, 1992). Concurrently, high aerosol loadings over the Indian subcontinent can be lofted and transported northward to the TP by monsoonal flow (Kang et al., 2019; Yu et al., 2024; Z. Zhao et al., 2013). These intrusions of aerosols and water vapor significantly influence cloud and precipitation processes over the TP and alter regional radiative forcing. The transport mechanism is primarily driven by strong SASM activity, which efficiently lifts pollutants from the Indian subcontinent into the upper-level anticyclone, thereby increasing aerosol concentrations in the upper troposphere over the TP (e.g., Fadnavis et al., 2013, 2017; J. Ma et al., 2019). However, the influence of low-level transport pathways remains uncertain. Specifically, whether stronger monsoon activity enhances aerosol transport and subsequently increases CCN activation capacity in the mid–lower troposphere over the TP is still unclear, limiting our understanding of cloud formation and aerosol–cloud interactions in this climatically sensitive region.

To address this, the GACPE-STP campaign was extended through a comprehensive in situ experiment at Mt. Qomolangma Station, covering the full 2024 monsoon season. The aims of the experiment are to examine whether the weak aerosol activation capacity observed over the southern TP (Y. Wang et al., 2024) persists throughout the entire monsoon period and explores how variations in SASM intensity influence the aerosol activation capacity in this region. These questions form the central focus of the present study.

2. Data and Methods

2.1. Experiment and Data

The Qomolangma Comprehensive Atmospheric and Environmental Observation Research Station of Chinese Academy of Sciences (QOMS; 28.21°N, 86.56°E, 4276 m a.s.l.) is located on the northern slope of Qomolangma, approximately 30 km from the Qomolangma Base Camp. The in situ experiment was conducted from 26 May to 25 September 2024, yielding 123 consecutive days of observations that fully covered the monsoon season. Situated in a pristine environment with minimal human activity and no industrial emissions, QOMS is representative of clean background conditions over the southern TP (Kang et al., 2022).

A site photo of the experiment is provided in Figure S1 in Supporting Information S1. To characterize aerosol activation capacity, the following instruments were employed. A CCN counter equipped with double cloud columns (CCNC, model 200; DMT Inc.) was used to quantify CCN number concentrations (N_{CCN}) at different water vapor supersaturation (SS) levels (Lance et al., 2006; Roberts & Nenes, 2005). Column A was operated at a constant SS of 0.2%, while Column B cycled through 9 SS levels ranging from 0.07% to 0.7%, completing one cycle approximately every hour. Unactivated particles at low SS were identified and corrected following the methodology of Y. Wang et al. (2019) and Tao et al. (2023). As shown in Figure S2a in Supporting Information S1, the N_{CCN} measured simultaneously by Columns A and B at 0.2% SS exhibited a strong positive correlation, with a Pearson correlation coefficient (r) of 1.00 and a slope of 1.18, supporting the reliability of the CCN measurements.

A Scanning Mobility Particle Sizer (SMPS, model 3938L50; TSI Inc.) measured the dry particle number size distribution (PNSD, 19.5–710.5 nm, 101 bins), and the total aerosol number concentration (N_a) was derived by integrating the entire PNSD. A full PNSD was obtained every 2 min. A comparison of N_a and N_{CCN} at 0.2% SS from Column A is shown in Figure S2b in Supporting Information S1. Driven by variations in SASM intensity, the relationship between N_a and N_{CCN} exhibits two distinct positive correlations with different slopes, as discussed in the Result Section.

A seven-wavelength Aethalometer (AE33, Magee Scientific Inc.) was employed to measure aerosol absorption coefficients and derive equivalent black carbon (BC) mass concentration (Drinovec et al., 2015). Meteorological parameters, including temperature, relative humidity (RH), pressure, wind direction and speed, and precipitation, were recorded by an automatic weather station (WXT530; Vaisala Inc.), with the temporal evolution of their daily averages shown in Figure S3 in Supporting Information S1. Additionally, monsoon indices characterizing SASM intensity are derived from NCEP reanalysis data. Aerosol loading and daily precipitation are represented using MODIS aerosol optical depth (AOD) products and GPM precipitation data, respectively.

2.2. Monsoon Index and HYSPLIT Model

The SASM intensity can be quantified using several established indices. In this study, we adopt the Onset Circulation Index (OCI) proposed by B. Wang et al. (2009) to characterize the evolution of the 2024 SASM. The OCI is defined as the average 850 hPa zonal wind over the southern Arabian Sea (5°–15°N, 40°–80°E), with the SASM onset identified when the index exceeds 6.2 m s^{-1} for at least seven consecutive days. In addition to the OCI, other commonly used indices were calculated, with definitions provided in Table S1 in Supporting Information S1. As shown in Figure S4 in Supporting Information S1, all indices consistently indicate that the 2024 SASM began in early June, reached its peak in July, and ended in late September. Significant correlations among these indices (Figure S5 in Supporting Information S1) suggest that the choice of index does not affect the robustness of our conclusions.

The HYSPLIT model (https://www.arl.noaa.gov/hysplit/, last access: 30 May 2025), developed by the Air Resources Laboratory of NOAA, was used to simulate the atmospheric transport of air masses (Stein et al., 2015). Following trajectory durations commonly used in the TP region (J. Xu et al., 2018; L. Zhang et al., 2021), 72-hr backward trajectories were computed at 1-hr intervals from a starting height of 100 m above ground level, resulting in 2,952 trajectories over the 123-day observation period. These trajectories were subsequently classified into four clusters.

3. Results

3.1. Low Aerosol Concentrations and Weak Activation Capacity

Figure 1 presents the time series of daily averaged aerosol physicochemical and activation characteristics throughout the campaign. The dry PNSD exhibited a unimodal pattern (Figure 1a). The daily-mean N_a ranged from 240 cm^{-3} to 1567 cm^{-3}, with an average of 732 cm^{-3}, which is comparable to those reported in the Amazon rainforest (Gunthe et al., 2009; Pöhlker et al., 2016). The daily-mean median particle diameter (D_{median}) averaged 73.7 nm, reaching a maximum of 126.8 nm and a minimum of 44.5 nm.

Time series of N_{CCN} under different SS conditions is shown in Figure 1c. Positive correlations are observed among N_{CCN} values across all SS levels. As SS increased from 0.07% to 0.7%, the average N_{CCN} rose from 7 to 238 cm^{-3}, and the corresponding activation fraction (AF, defined as the ratio of N_{CCN} to N_a) increased from 0.7% to 32.4%. At a SS of 0.2%, the daily-mean N_{CCN} varied from 5 to 282 cm^{-3} with an average of 52 cm^{-3}. The corresponding daily-mean AF ranged from 1.6% to 18.3%, averaging 6.2%. The dependence of N_{CCN} on SS follows a power-law relationship:

$$N_{CCN} = C \times SS^{k} \quad (1)$$

where the fitted coefficient C is 371 cm^{-3}, representing the N_{CCN} at 1% SS, and the exponent k is 1.05, exceeding the typical continental range of 0.4–0.9 summarized by Seinfeld and Pandis (2016). Figure 1d shows the time series of the aerosol hygroscopicity parameter (κ) at 0.2% SS, derived from N_{CCN} and the dry PNSD based on κ-Köhler theory (Petters & Kreidenweis, 2007; see Text S1 in Supporting Information S1 for calculation details). The κ values obtained from CCNC Columns A and B were 0.06 and 0.07, respectively, indicating weak aerosol hygroscopicity. These values are substantially lower than the continental reference value of 0.3, as recommended by Andreae and Rosenfeld (2008).

Compared to observations at the Yadong site (Y. Wang et al., 2024), the present experiment at QOMS revealed even lower aerosol concentration and weaker activation capacity. Specifically, lower N_a (732 vs. 962 cm^{-3}), smaller D_{median} (73.7 vs. 93 nm), and reduced κ (0.07 vs. 0.09 at 0.2% SS) were observed at QOMS. These factors

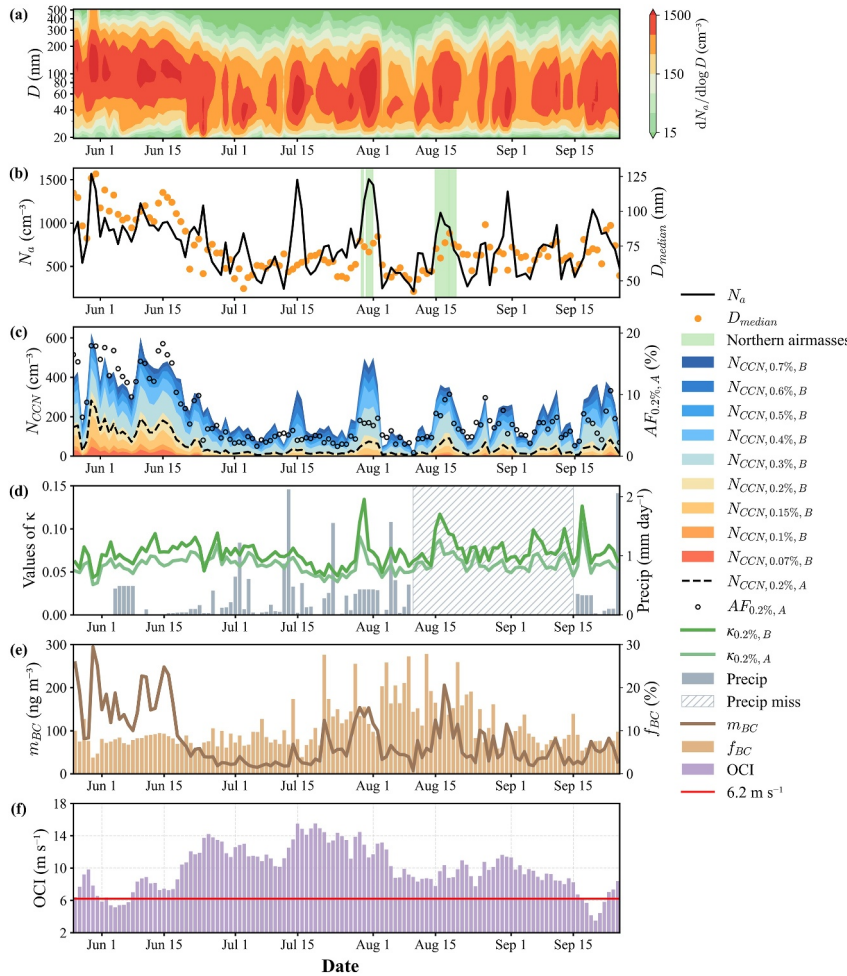

Figure 1. Time series of daily-mean aerosol physicochemical and activation characteristics and South Asian summer monsoon index during the observation period. (a) PNSD, (b) N_a and D_{median}, (c) N_{CCN} at various SS conditions, and activation fraction at 0.2% SS, (d) κ and daily precipitation, (e) m_{BC} and f_{BC}, (f) the Onset Circulation Index.

led to significantly lower N_{CCN} (52 vs. 206 cm^{-3} at 0.2% SS) and AF (6.2% vs. 14.7% at 0.2% SS) at QOMS, indicating a further suppression of aerosol activation. Despite a nearly 1 km difference in altitude and slightly different observation periods, the similar results observed at the two sites highlight the generally weak ability of aerosols to activate as cloud droplets in southern TP during the SASM period.

A notable feature in the time series of aerosol activation characteristics is the significantly stronger activation capacity observed during the early part of the campaign, prior to mid-June. This period is characterized by larger D_{median} and higher N_a, N_{CCN}, and AF. On average, both AF and N_{CCN} before mid-June were approximately 3.5 and 5 times higher, respectively, than those after mid-June. This contrast also explains the two distinct positive slopes in the correlation between N_a and N_{CCN} shown in Figure S2b in Supporting Information S1. In addition, as shown in Figure 1e, the BC mass concentration (m_{BC}) exhibited a temporal pattern similar to that of N_a and N_{CCN}, with higher values observed before mid-June and a noticeable decrease thereafter. However, the BC mass fraction (f_{BC}, defined as the ratio of m_{BC} to total aerosol mass concentration) increased after mid-June, especially following mid-July. The underlying mechanism is closely linked to variations in SASM intensity and is discussed in subsequent sections.

3.2. SASM Weakens Aerosol Activation Capacity

Driven by the SASM, aerosols from the Indian subcontinent and moisture from the Indian Ocean and the Bay of Bengal are transported northward to the TP (Guo et al., 2025; Yu et al., 2024; Z. Zhao et al., 2013). Building on

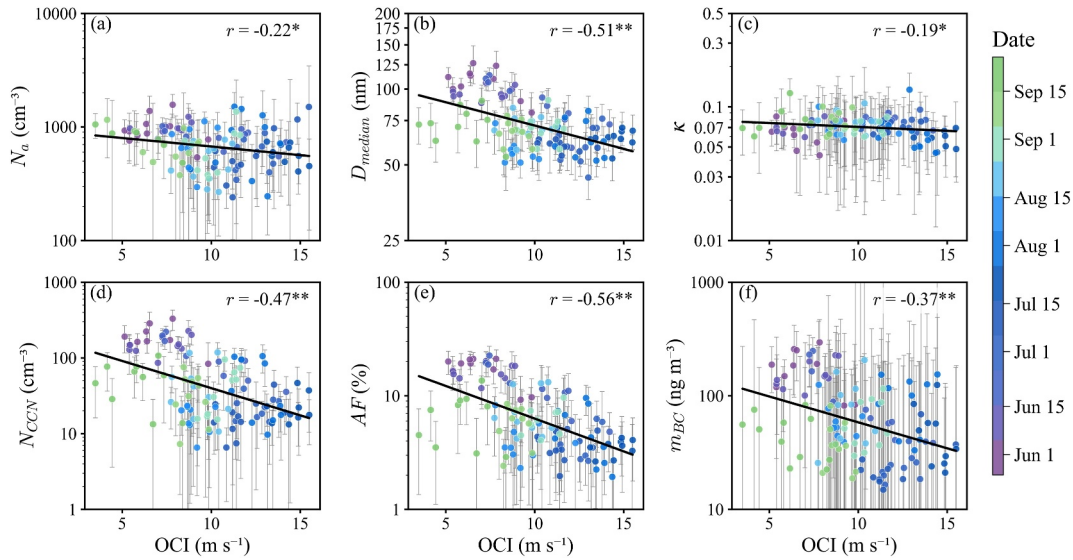

Figure 2. Correlations between onset circulation index and daily-mean aerosol physicochemical and activation characteristics: (a) N_a, (b) D_{median}, (c) κ, (d) N_{CCN} at 0.2% supersaturation, (e) activation fraction at 0.2% supersaturation, (f) m_{BC}. Error bar represents one standard deviation. Color bar indicates date, and black lines represent linear fits. Asterisks denote significance levels determined through weighted least squares (*$p < 0.05$, **$p < 0.01$).

this, we investigate how variations in SASM intensity influence the aerosol activation capacity in the lower troposphere over the southern TP. The strength of the 2024 SASM is characterized using the OCI (B. Wang et al., 2009), and its temporal evolution during the observation period is shown in Figure 1f. The influx of moisture transported by the monsoon led to a marked increase in RH at QOMS, with its temporal variability broadly consistent with the SASM intensity (Figures S3b and S6 in Supporting Information S1).

Figure 2 presents the correlations between the OCI and daily-mean aerosol physicochemical and activation characteristics. First, OCI shows a weak but statistically significant negative correlation with N_a ($r = -0.22$), passing the 95% confidence level. This indicates that, contrary to expectations, stronger monsoonal transport does not increase N_a over the TP but rather decreases N_a. Second, a significant negative correlation is found between OCI and D_{median} ($r = -0.51$), passing the 99% confidence level, suggesting that stronger monsoons are associated with a reduction in larger aerosol particles over the TP. Third, OCI exhibits a weak negative correlation with κ ($r = -0.19$), also significant at the 95% level, implying a decline in aerosol hygroscopicity under stronger monsoon conditions. Together, the negative correlations between OCI and N_a, D_{median}, and κ explain the overall reduction in aerosol concentration and activation capacity with increasing SASM intensity. As shown in Figures 2d and 2e, both N_{CCN} and AF at 0.2% SS exhibit significant negative correlations with OCI ($r = -0.47$ and -0.56, respectively), exceeding the 99% confidence level. We select N_{CCN} and AF at 0.2% SS as representative metrics, as previous in situ observations from the GACPE-STP campaign identified 0.2% as the characteristic peak effective SS within orographic clouds over the southern TP (Y. Wang et al., 2025). Similar significant negative correlations between OCI and N_{CCN} and AF are observed at other SS levels (Figures S7 and S8 in Supporting Information S1). In addition, the m_{BC} also shows a negative correlation with OCI ($r = -0.37$), significant at the 99% confidence level (Figure 2f). However, the strength of this correlation is weaker than that between OCI and N_{CCN} at any SS level, as indicated by a lower r.

3.3. Underlying Mechanisms

Backward trajectory simulations using the HYSPLIT model reveal that during the observation period, approximately 94% of air masses arriving at QOMS originated from the low-altitude Indian subcontinent, while 5% and 1% were traced to the central TP and the Taklimakan Desert, respectively (Figure 3a). Figure 3b shows all simulated trajectories overlaid on the MODIS AOD field. Northeastern India exhibits substantially elevated AOD compared to surrounding regions, primarily due to intensive emissions from residential and transportation sources (Dutta & Chatterjee, 2022). Driven by the SASM, aerosols from these highly polluted areas may be transported

10.1029/2025GL118406

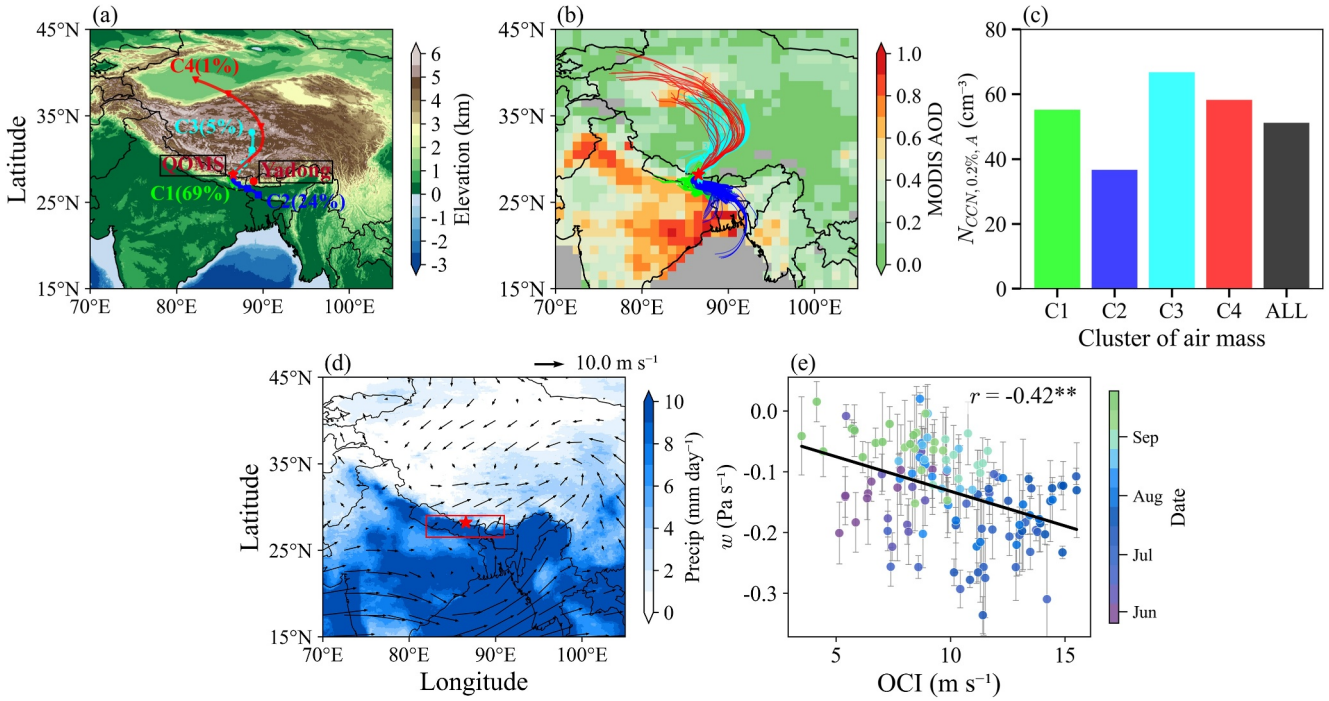

Figure 3. Topography of the Tibetan Plateau and surrounding regions, background aerosol loading, precipitation distribution, and air mass trajectories during the observation period at QOMS. (a) Location of QOMS, with colored lines indicating clustered 72-hr HYSPLIT backward trajectories; (b) all trajectories overlaid on the mean MODIS aerosol optical depth (AOD; gray indicates missing data); (c) mean N_{CCN} at 0.2% supersaturation under different trajectory clusters, with black bars indicating the overall mean; (d) daily precipitation derived from GPM and mean wind vectors from NCEP reanalysis; (e) correlation between onset circulation index and vertical velocity (w) averaged over the red box area in panel (d) at 750 hPa.

toward the TP. In contrast, air masses from northern pathways traverse regions characterized by relatively low AOD levels and are dominated by dust aerosols, which typically contribute only minimally to CCN formation (Chen et al., 2020; Manktelow et al., 2010). Interestingly, in situ measurements show that air masses from the north are associated with slightly higher N_{CCN} values than those from the more polluted southern regions (Figure 3c).

This pattern is closely associated with the frequent precipitation along the southern slope of the TP (Figure 3d). During the SASM, monsoonal air masses are orographically lifted by the terrain, triggering cloud formation and subsequent precipitation. In this process, particles with higher activation potential are preferentially removed, leaving behind smaller and less hygroscopic aerosols. Activation as cloud droplets does not directly remove aerosols, due to the complexities of cloud processing, while precipitation-related scavenging (e.g., below-cloud scavenging, in-cloud coalescence) reduces aerosol concentrations. Although these air masses initially carry abundant moisture and aerosols, their ascent over the southern TP slope leads to significant CCN consumption and aerosol reduction, weakening their activation capacity by the time they reach QOMS. In contrast, air masses from the north, dominated by dust aerosols and traveling through regions with limited cloud development and precipitation, retain relatively higher activation capacity.

The orographic lifting of monsoonal air masses also accounts for the observed negative correlation between SASM intensity, as represented by the OCI, and aerosol activation capacity. On days with stronger monsoon activity, enhanced vertical ascent over the southern TP slope leads to rapid lifting and cooling of air parcels (Figure 3e). This favors higher SS levels, promotes CCN activation as clouds, and accelerates cloud microphysical processes such as condensation and collision–coalescence, ultimately resulting in increased precipitation. These conditions enhance the depletion of effective CCN and intensify aerosol removal through wet scavenging, thereby reducing the aerosol activation capacity at QOMS.

BC is generally hydrophobic or weakly hygroscopic (Laborde et al., 2013; Peng et al., 2017), but its mixing state can allow activation under sufficient water vapor (Hu et al., 2021; Kuang et al., 2024; Motos et al., 2019;

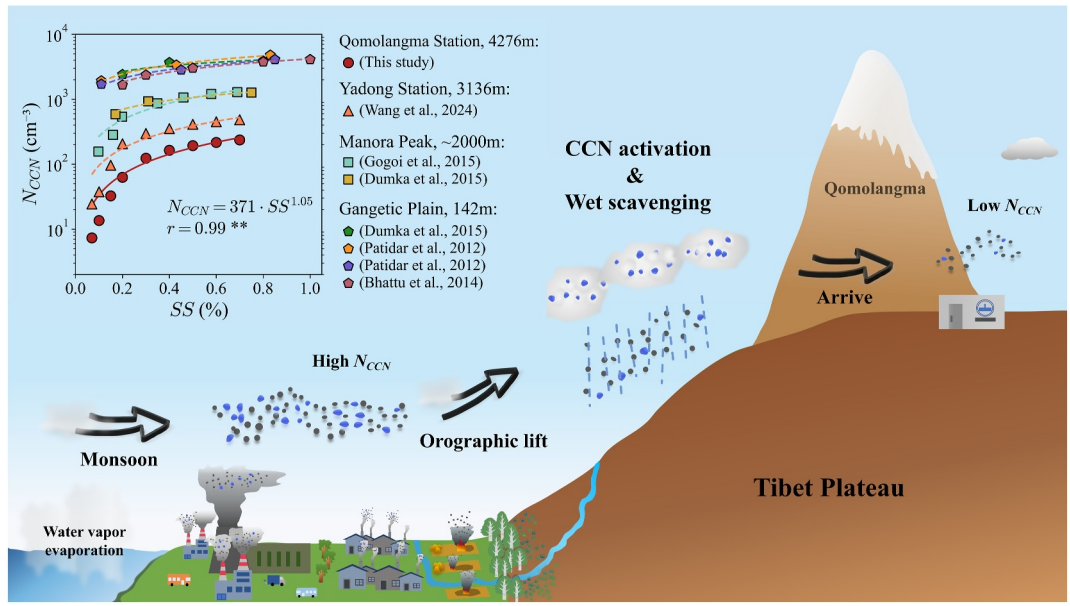

Figure 4. Schematic illustration of the mechanism by which the South Asian summer monsoon suppresses aerosols activation as cloud droplets over the southern Tibetan Plateau (TP). The subplots show the dependence of N_{CCN} on SS observed at sites located at different altitudes over the southern TP and the Indian subcontinent.

Tian et al., 2024). The observed negative correlation between OCI and m_{BC} reflects the combined effects of in-cloud processing and wet scavenging during transport. Generally, weaker activation of BC-containing aerosols generally leads to weaker scavenging, but it remains uncertain whether sub-cloud scavenging dominates. The increase in f_{BC} during the later phase of the SASM (Figure 1e) suggests that particles with higher activation potential are more likely to be removed by cloud processes, leaving a relatively higher fraction of BC at QOMS.

Furthermore, CCN measurements from observation stations at different elevations along the transport pathway from the Indian subcontinent to the southern TP during the SASM consistently show a pronounced decline in N_{CCN} with increasing altitude (Figure 4). At 0.2% SS, the mean N_{CCN} values are reported to be approximately 2000 cm^{-3} at the Indo-Gangetic Plain station (142 m; Dumka et al., 2015; Patidar et al., 2012; Bhattu & Tripathi, 2014), around 550 cm^{-3} at Mt. Marora station (~2 km; Gogoi et al., 2015; Dumka et al., 2015), and 206 cm^{-3} at Yadong Station (3136 m; Y. Wang et al., 2024). In this study, an even lower value of 52 cm^{-3} is observed at QOMS (4276 m). This vertical gradient in N_{CCN} supports the proposed mechanism that monsoonal air masses, as they are lifted along the southern TP slope, experience substantial CCN depletion due to cloud formation and precipitation scavenging, thereby reducing their aerosol activation capacity upon arrival at the Plateau. Nevertheless, further down the mountain, the relationship between SASM intensity and aerosol activation capacity could be different, which warrants discussion in future studies.

4. Conclusions and Discussions

Tibetan Plateau plays a critical role in regulating regional hydrological cycles, radiative energy balance, and large-scale climate. However, aerosol–cloud interactions over this high-altitude region remain poorly constrained due to limited in situ observations, particularly in terms of aerosols activation as clouds. The SASM transports pollutants from the Indian subcontinent to the upper troposphere over the TP (Fadnavis et al., 2017; X. Zhang et al., 2025). However, due to limited observational evidence, it remains unclear whether the SASM can transport pollutants into the lower troposphere over the TP and, consequently, how this affects aerosol activation capacity. Thus, we conducted a comprehensive in situ experiment at the QOMS on the southern TP, covering the full 2024 SASM period.

We observed generally weak aerosol activation capacity at QOMS. The mean N_{CCN} increased from 7 to 238 cm^{-3} as the SS increased from 0.07% to 0.7%. The κ remained consistently below 0.1. These findings are consistent

with in situ observations at the Yadong site during the latter half of the 2023 monsoon season (Y. Wang et al., 2024), indicating that weak CCN activation may be a persistent feature over the southern TP during the monsoon.

In addition to the influence of local emissions, this study identifies a clear suppressive influence of the SASM on aerosol activation capacity over the southern TP. The OCI, used to quantify SASM intensity, shows significant negative correlations with N_a, D_{median}, κ, N_{CCN}, and AF. Previous studies show that strong SASM activity efficiently lifts pollutants from the Indian subcontinent into the upper-level anticyclone, increasing aerosol concentrations in the TP upper troposphere (e.g., Fadnavis et al., 2013, 2017; J. Ma et al., 2019; X. Zhang et al., 2025). In contrast, our results reveal that more intense monsoon conditions are instead associated with a reduced aerosol concentrations and activation capacity in the lower troposphere over the southern TP. As illustrated schematically in Figure 4, this inverse relationship can be explained by the orographic lifting of moist monsoonal air masses along the southern TP slope. As these air masses ascend, cooling increases the SS, promoting CCN activation and accelerating warm-cloud microphysical processes such as condensation and collision–coalescence. These processes enhance precipitation development, which in turn leads to significant aerosol removal via wet scavenging. As a result, both N_a and N_{CCN} are substantially depleted by the time these air parcels reach the QOMS site. Moreover, stronger SASM conditions are associated with enhanced vertical velocities over the southern TP slope, further intensifying in-cloud activation and wet removal processes.

These results highlight the significant influence of the SASM on aerosol activation as clouds into the lower troposphere over the southern TP. While this study focuses on CCN and liquid-phase clouds, the response of ice-nucleating particles (INPs) under similar conditions remains uncertain. Given the prevalence of mixed-phase and ice clouds over the TP (J. Wang et al., 2021), future campaigns should integrate simultaneous CCN and INP measurements to better constrain aerosol–cloud interactions in this climatically sensitive region.

Conflict of Interest

The authors declare no conflicts of interest relevant to this study.

Data Availability Statement

Data used in this study are available from Ji et al. (2025).

Acknowledgments
This research is supported by the NSFC Regional Innovation and Development Joint Fund (U24A20604), the National Natural Science Foundation of China (42575074, 42205072), the Second Tibetan Plateau Scientific Expedition and Research Program (2019QZKK0602), and the Fundamental Research Funds for the Central Universities (lzujbky-2025-jdzx01).

References

Andreae, M. O., & Rosenfeld, D. (2008). Aerosol–cloud–precipitation interactions. Part 1. The nature and sources of cloud-active aerosols. *Earth-Science Reviews*, *89*(1–2), 13–41. https://doi.org/10.1016/j.earscirev.2008.03.001

Bhattu, D., & Tripathi, S. N. (2014). Inter-seasonal variability in size-resolved CCN properties at Kanpur, India. *Atmospheric Environment*, *85*, 161–168. https://doi.org/10.1016/j.atmosenv.2013.12.016

Bougiatioti, A., Bezantakos, S., Stavroulas, I., Kalivitis, N., Kokkalis, P., Biskos, G., et al. (2016). Biomass-burning impact on CCN number, hygroscopicity and cloud formation during summertime in the eastern Mediterranean. *Atmospheric Chemistry and Physics*, *16*(11), 7389–7409. https://doi.org/10.5194/acp-16-7389-2016

Charlson, R. J., Schwartz, S. E., Hales, J. M., Cess, R. D., Coakley Jr, J. A., Hansen, J. E., & Hofmann, D. J. (1992). Climate forcing by anthropogenic aerosols. *Science*, *255*(5043), 423–430. https://doi.org/10.1126/science.255.5043.423

Chen, L., Peng, C., Gu, W., Fu, H., Jian, X., Zhang, H., et al. (2020). On mineral dust aerosol hygroscopicity. *Atmospheric Chemistry and Physics*, *20*(21), 13611–13626. https://doi.org/10.5194/acp-20-13611-2020

Deng, Z., Zhao, C., Ma, N., Liu, P., Ran, L., Xu, W., et al. (2011). Size-resolved and bulk activation properties of aerosols in the North China Plain. *Atmospheric Chemistry and Physics*, *11*(8), 3835–3846. https://doi.org/10.5194/acp-11-3835-2011

Drinovec, L., Močnik, G., Zotter, P., Prévôt, A. S. H., Ruckstuhl, C., Coz, E., et al. (2015). The "dual-spot" aethalometer: An improved measurement of aerosol black carbon with real-time loading compensation. *Atmospheric Measurement Techniques*, *8*(5), 1965–1979. https://doi.org/10.5194/amt-8-1965-2015

Dumka, U. C., Bhattu, D., Tripathi, S. N., Kaskaoutis, D. G., & Madhavan, B. L. (2015). Seasonal inhomogeneity in cloud precursors over Gangetic Himalayan region during GVAX campaign. *Atmospheric Research*, *155*, 158–175. https://doi.org/10.1016/j.atmosres.2014.11.022

Dutta, M., & Chatterjee, A. (2022). A deep insight into state-level aerosol pollution in India: Long-term (2005–2019) characteristics, source apportionment, and future projection (2023). *Atmospheric Environment*, *289*, 119312. https://doi.org/10.1016/j.atmosenv.2022.119312

Fadnavis, S., Kalita, G., Kumar, K. R., Gasparini, B., & Li, J. (2017). Potential impact of carbonaceous aerosol on the upper troposphere and lower stratosphere (UTLS) and precipitation during Asian summer monsoon in a global model simulation. *Atmospheric Chemistry and Physics*, *17*(18), 11637–11654. https://doi.org/10.5194/acp-17-11637-2017

Fadnavis, S., Semeniuk, K., Pozzoli, L., Schultz, M. G., Ghude, S. D., Das, S., & Kakatkar, R. (2013). Transport of aerosols into the UTLS and their impact on the Asian monsoon region as seen in a global model simulation. *Atmospheric Chemistry and Physics*, *13*(17), 8771–8786. https://doi.org/10.5194/acp-13-8771-2013

Gogoi, M. M., Babu, S. S., Jayachandran, V., Moorthy, K. K., Satheesh, S. K., Naja, M., & Kotamarthi, V. R. (2015). Optical properties and CCN activity of aerosols in a high-altitude Himalayan environment: Results from RAWEX-GVAX. *Journal of Geophysical Research: Atmospheres*, *120*(6), 2453–2469. https://doi.org/10.1002/2014JD022966

Gong, X., Wex, H., Müller, T., Wiedensohler, A., Höhler, K., Kandler, K., et al. (2019). Characterization of aerosol properties at Cyprus, focusing on cloud condensation nuclei and ice-nucleating particles. *Atmospheric Chemistry and Physics*, *19*(16), 10883–10900. https://doi.org/10.5194/acp-19-10883-2019

Gunthe, S. S., King, S. M., Rose, D., Chen, Q., Roldin, P., Farmer, D. K., et al. (2009). Cloud condensation nuclei in pristine tropical rainforest air of Amazonia: Size-resolved measurements and modeling of atmospheric aerosol composition and CCN activity. *Atmospheric Chemistry and Physics*, *9*(19), 7551–7575. https://doi.org/10.5194/acp-9-7551-2009

Guo, X., Wang, L., Tian, L., Zhang, L., & Zhao, W. (2025). Quantitative identification of moisture sources over the Tibetan Plateau: Spatial distributions and temporal variabilities. *Journal of Climate*, *38*(1), 263–276. https://doi.org/10.1175/jcli-d-24-0093.1

Hu, D., Liu, D., Kong, S., Zhao, D., Wu, Y., Li, S., et al. (2021). Direct quantification of droplet activation of ambient Black carbon under water supersaturation. *Journal of Geophysical Research: Atmospheres*, *126*(13), e2021JD034649. https://doi.org/10.1029/2021JD034649

Irwin, M., Robinson, N., Allan, J. D., Coe, H., & McFiggans, G. (2011). Size-resolved aerosol water uptake and cloud condensation nuclei measurements as measured above a Southeast Asian rainforest during OP3. *Atmospheric Chemistry and Physics*, *11*(21), 11157–11174. https://doi.org/10.5194/acp-11-11157-2011

Jayachandran, V., Nair, V. S., & Babu, S. S. (2018). CCN activation properties at a tropical hill station in Western Ghats during south-west summer monsoon: Vertical heterogeneity. *Atmospheric Research*, *214*, 36–45. https://doi.org/10.1016/j.atmosres.2018.07.018

Ji, Z., Wang, Y., & Li, J. (2025). In-situ observations reveal South Asian Summer Monsoon weakens Aerosols Activation into Clouds over Southern Tibetan Plateau [Dataset]. *Zenodo*. https://doi.org/10.5281/zenodo.17920482

Kang, S., Zhang, Q., Qian, Y., Ji, Z., Li, C., Cong, Z., et al. (2019). Linking atmospheric pollution to cryospheric change in the Third Pole region: Current progress and future prospects. *National Science Review*, *6*(4), 796–809. https://doi.org/10.1093/nsr/nwz031

Kang, S., Zhang, Q., Zhang, Y., Guo, W., Ji, Z., Shen, M., et al. (2022). Warming and thawing in the Mt. Everes of climate and environmental changes. *Earth-Science Reviews*, *225*, 103911. https://doi.org/10.1016/j.earscirev.2021.103911

Kuang, Y., Xu, W., Tao, J., Luo, B., Liu, L., Xu, H., et al. (2024). Divergent impacts of biomass burning and fossil fuel combustion aerosols on fog-cloud microphysics and chemistry: Novel insights from advanced aerosol-fog sampling. *Geophysical Research Letters*, *51*(4), e2023GL107147. https://doi.org/10.1029/2023GL107147

Laborde, M., Crippa, M., Tritscher, T., Jurányi, Z., Decarlo, P. F., Temime-Roussel, B., et al. (2013). Black carbon physical properties and mixing state in the European megacity Paris. *Atmospheric Chemistry and Physics*, *13*(11), 5831–5856. https://doi.org/10.5194/acp-13-5831-2013

Lance, S., Nenes, A., Medina, J., & Smith, J. N. (2006). Mapping the operation of the DMT continuous flow CCN counter. *Aerosol Science and Technology*, *40*(4), 242–254. https://doi.org/10.1080/02786820500543290

Liu, Y., Lu, M., Yang, H., Duan, A., He, B., Yang, S., & Wu, G. (2020). Land–atmosphere–ocean coupling associated with the Tibetan Plateau and its climate impacts. *National Science Review*, *7*(3), 534–552. https://doi.org/10.1093/nsr/nwaa011

Ma, J., Brühl, C., He, Q., Steil, B., Karydis, V. A., Klingmüller, K., et al. (2019). Modeling the aerosol chemical composition of the tropopause over the Tibetan Plateau during the Asian summer monsoon. *Atmospheric Chemistry and Physics*, *19*(17), 11587–11612. https://doi.org/10.5194/acp-19-11587-2019

Ma, Y., Ma, W., Zhong, L., Hu, Z., Li, M., Zhu, Z., et al. (2017). Monitoring and modeling the Tibetan Plateau's climate system and its impact on East Asia. *Scientific Reports*, *7*(1), 44574. https://doi.org/10.1038/srep44574

Manktelow, P. T., Carslaw, K. S., Mann, G. W., & Spracklen, D. V. (2010). The impact of dust on sulfate aerosol, CN and CCN during an East Asian dust storm. *Atmospheric Chemistry and Physics*, *10*(2), 365–382. https://doi.org/10.5194/acp-10-365-2010

Motos, G., Schmale, J., Corbin, J. C., Zanatta, M., Baltensperger, U., & Gysel-Beer, M. (2019). Droplet activation behaviour of atmospheric black carbon particles in fog as a function of their size and mixing state. *Atmospheric Chemistry and Physics*, *19*(4), 2183–2207. https://doi.org/10.5194/acp-19-2183-2019

Patidar, V., Tripathi, S. N., Bharti, P. K., & Gupta, T. (2012). First surface measurement of cloud condensation nuclei over Kanpur, IGP: Role of long range transport. *Aerosol Science and Technology*, *46*(9), 973–982. https://doi.org/10.1080/02786826.2012.685113

Peng, J., Hu, M., Guo, S., Du, Z., Shang, D., Zheng, J., et al. (2017). Ageing and hygroscopicity variation of black carbon particles in Beijing measured by a quasi-atmospheric aerosol evolution study (QUALITY) chamber. *Atmospheric Chemistry and Physics*, *17*(17), 10333–10348. https://doi.org/10.5194/acp-17-10333-2017

Petters, M. D., & Kreidenweis, S. M. (2007). A single parameter representation of hygroscopic growth and cloud condensation nucleus activity. *Atmospheric Chemistry and Physics*, *7*(8), 1961–1971. https://doi.org/10.5194/acp-7-1961-2007

Pöhlker, M. L., Pöhlker, C., Ditas, F., Klimach, T., Hrabe De Angelis, I., Araújo, A., et al. (2016). Long-term observations of cloud condensation nuclei in the Amazon rain forest – Part 1: Aerosol size distribution, hygroscopicity, and new model parametrizations for CCN prediction. *Atmospheric Chemistry and Physics*, *16*(24), 15709–15740. https://doi.org/10.5194/acp-16-15709-2016

Pöhlker, M. L., Pöhlker, C., Quaas, J., Mülmenstädt, J., Pozzer, A., Andreae, M. O., et al. (2023). Global organic and inorganic aerosol hygroscopicity and its effect on radiative forcing. *Nature Communications*, *14*(1), 6139. https://doi.org/10.1038/s41467-023-41695-8

Prabhakaran, P., Shawon, A. S. M., Kinney, G., Thomas, S., Cantrell, W., & Shaw, R. A. (2020). The role of turbulent fluctuations in aerosol activation and cloud formation. *Proceedings of the National Academy of Sciences*, *117*(29), 16831–16838. https://doi.org/10.1073/pnas.2006426117

Rejano, F., Casans, A., Via, M., Casquero-Vera, J. A., Castillo, S., Lyamani, H., et al. (2024). CCN estimations at a high-altitude remote site: Role of organic aerosol variability and hygroscopicity. *Atmospheric Chemistry and Physics*, *24*(24), 13865–13888. https://doi.org/10.5194/acp-24-13865-2024

Rejano, F., Titos, G., Casquero-Vera, J. A., Lyamani, H., Andrews, E., Sheridan, P., et al. (2021). Activation properties of aerosol particles as cloud condensation nuclei at urban and high-altitude remote sites in southern Europe. *Science of The Total Environment*, *762*, 143100. https://doi.org/10.1016/j.scitotenv.2020.143100

Roberts, G. C., & Nenes, A. (2005). A continuous-flow streamwise thermal-gradient CCN chamber for atmospheric measurements. *Aerosol Science and Technology*, *39*(3), 206–221. https://doi.org/10.1080/027868290913988

Salma, I., Thén, W., Vörösmarty, M., & Gyöngyösi, A. Z. (2021). Cloud activation properties of aerosol particles in a continental Central European urban environment. *Atmospheric Chemistry and Physics*, *21*(14), 11289–11302. https://doi.org/10.5194/acp-21-11289-2021

Seinfeld, J. H., & Pandis, S. N. (2016). *Atmospheric chemistry and physics: From air pollution to climate change*. John Wiley.

Shen, X., Liu, Q., Sun, J., Kong, W., Ma, Q., Qi, B., et al. (2025). Measurement report: The influence of particle number size distribution and hygroscopicity on the microphysical properties of cloud droplets at a mountain site. *Atmospheric Chemistry and Physics*, *25*(11), 5711–5725. https://doi.org/10.5194/acp-25-5711-2025

Singla, V., Mukherjee, S., Safai, P. D., Meena, G. S., Dani, K. K., & Pandithurai, G. (2017). Role of organic aerosols in CCN activation and closure over a rural background site in Western Ghats, India. *Atmospheric Environment*, *158*, 148–159. https://doi.org/10.1016/j.atmosenv.2017.03.037

Stein, A. F., Draxler, R. R., Rolph, G. D., Stunder, B. J. B., Cohen, M. D., & Ngan, F. (2015). NOAA's HYSPLIT atmospheric transport and dispersion modeling system. *Bulletin of the American Meteorological Society*, *96*(12), 2059–2077. https://doi.org/10.1175/bams-d-14-00110.1

Stevens, B., & Feingold, G. (2009). Untangling aerosol effects on clouds and precipitation in a buffered system. *Nature*, *461*(7264), 607–613. https://doi.org/10.1038/nature08281

Stier, P., Van Den Heever, S. C., Christensen, M. W., Gryspeerdt, E., Dagan, G., Saleeby, S. M., et al. (2024). Multifaceted aerosol effects on precipitation. *Nature Geoscience*, *17*(8), 719–732. https://doi.org/10.1038/s41561-024-01482-6

Tao, J., Kuang, Y., Luo, B., Liu, L., Xu, H., Ma, N., et al. (2023). Kinetic limitations affect cloud condensation nuclei activity measurements under low supersaturation. *Geophysical Research Letters*, *50*(4), e2022GL101603. https://doi.org/10.1029/2022gl101603

Tao, J., Kuang, Y., Ma, N., Hong, J., Sun, Y., Xu, W., et al. (2021). Secondary aerosol formation alters CCN activity in the North China Plain. *Atmospheric Chemistry and Physics*, *21*(9), 7409–7427. https://doi.org/10.5194/acp-21-7409-2021

Tian, P., Liu, D., Hu, K., Wu, Y., Huang, M., He, H., et al. (2024). Efficient droplet activation of ambient black carbon particles in a suburban environment. *Atmospheric Chemistry and Physics*, *24*(8), 5149–5164. https://doi.org/10.5194/acp-24-5149-2024

Wang, B., Ding, Q., & Joseph, P. V. (2009). Objective definition of the Indian summer monsoon onset. *Journal of Climate*, *22*(12), 3303–3316. https://doi.org/10.1175/2008JCLI2675.1

Wang, J., Jian, B., Wang, G., Zhao, Y., Li, Y., Letu, H., et al. (2021). Climatology of cloud phase, cloud radiative effects and precipitation properties over the Tibetan Plateau. *Remote Sensing*, *13*(3), 363. https://doi.org/10.3390/rs13030363

Wang, Y., Fang, F., Li, J., Zhang, P., Ji, Z., Shi, J., & Huang, J. (2025). High effective supersaturation offsets low aerosol hygroscopicity to promote orographic cloud formation over the southern Tibetan Plateau. *npj Climate and Atmospheric Science*, *8*(1), 231. https://doi.org/10.1038/s41612-025-01119-4

Wang, Y., Henning, S., Poulain, L., Lu, C., Stratmann, F., Wang, Y., et al. (2022). Aerosol activation characteristics and prediction at the central European ACTRIS research station of Melpitz, Germany. *Atmospheric Chemistry and Physics*, *22*(24), 15943–15962. https://doi.org/10.5194/acp-22-15943-2022

Wang, Y., Li, J., Fang, F., Zhang, P., He, J., Pöhlker, M. L., et al. (2024). In-situ observations reveal weak hygroscopicity in the Southern Tibetan Plateau: Implications for aerosol activation and indirect effects. *npj Climate and Atmospheric Science*, *7*(1), 77. https://doi.org/10.1038/s41612-024-00629-x

Wang, Y., Niu, S., Lv, J., Lu, C., Xu, X., Wang, Y., et al. (2019). A new method for distinguishing unactivated particles in cloud condensation nuclei measurements: Implications for aerosol indirect effect evaluation. *Geophysical Research Letters*, *46*(23), 14185–14194. https://doi.org/10.1029/2019GL085379

Webster, P. J., & Yang, S. (1992). Monsoon and ENSO: Selectively interactive systems. *Quarterly Journal of the Royal Meteorological Society*, *118*(507), 877–926. https://doi.org/10.1002/qj.49711850705

Xu, J., Zhang, Q., Shi, J., Ge, X., Xie, C., Wang, J., et al. (2018). Chemical characteristics of submicron particles at the central Tibetan Plateau: Insights from aerosol mass spectrometry. *Atmospheric Chemistry and Physics*, *18*(1), 427–443. https://doi.org/10.5194/acp-18-427-2018

Xu, J. Z., Mei, F., Zhang, X. H., Zhao, W. H., Zhai, L. X., Zhong, M., & Hou, S. G. (2024). Impact of anthropogenic aerosol transport on cloud condensation nuclei activity during summertime in Qilian Mountain, in the Northern Tibetan Plateau. *Journal of Geophysical Research: Atmospheres*, *129*(9), e2023JD040519. https://doi.org/10.1029/2023jd040519

Yu, Z., Tian, P., Kang, C., Song, X., Huang, J., Guo, Y., et al. (2024). Physical properties, chemical components, and transport mechanisms of atmospheric aerosols over a remote area on the south slope of the Tibetan Plateau. *Journal of Geophysical Research: Atmospheres*, *129*(4), e2023JD040193. https://doi.org/10.1029/2023JD040193

Yuan, L., & Zhao, C. (2023). Quantifying particle-to-particle heterogeneity in aerosol hygroscopicity. *Atmospheric Chemistry and Physics*, *23*(5), 3195–3205. https://doi.org/10.5194/acp-23-3195-2023

Zhang, L., Tang, C., Huang, J., Du, T., Guan, X., Tian, P., et al. (2021). Unexpected high absorption of atmospheric aerosols over a western Tibetan Plateau site in summer. *Journal of Geophysical Research: Atmospheres*, *126*(7), e2020JD033286. https://doi.org/10.1029/2020jd033286

Zhang, X., Xu, W., Song, X., Duan, X., Peng, X., Lin, W., et al. (2025). Cross-regional horizontal and vertical transport pathways of carbon monoxide and its impact on air pollution in the Tibetan Plateau. *Journal of Geophysical Research: Atmospheres*, *130*(5), e2024JD041859. https://doi.org/10.1029/2024JD041859

Zhao, C., Sun, Y., Yang, J., Li, J., Zhou, Y., Yang, Y., et al. (2024). Observational evidence and mechanisms of aerosol effects on precipitation. *Science Bulletin*, *69*(10), 1569–1580. https://doi.org/10.1016/j.scib.2024.03.014

Zhao, Z., Cao, J., Shen, Z., Xu, B., Zhu, C., Chen, L.-W. A., et al. (2013). Aerosol particles at a high-altitude site on the Southeast Tibetan Plateau, China: Implications for pollution transport from South Asia. *Journal of Geophysical Research: Atmospheres*, *118*(19), 11360–11375. https://doi.org/10.1002/jgrd.50599

References From the Supporting Information

Dusek, U., Frank, G. P., Hildebrandt, L., Curtius, J., Schneider, J., Walter, S., et al. (2006). Size matters more than chemistry for cloud-nucleating ability of aerosol particles. *Science*, *312*(5778), 1375–1378. https://doi.org/10.1126/science.1125261

Goswami, B. N., Krishnamurthy, V., & Annmalai, H. (1999). A broad-scale circulation index for the interannual variability of the Indian summer monsoon. *Quarterly Journal of the Royal Meteorological Society*, *125*(554), 611–633. https://doi.org/10.1002/qj.49712555412

Nenes, A., Charlson, R. J., Facchini, M. C., Kulmala, M., Laaksonen, A., & Seinfeld, J. H. (2002). Can chemical effects on cloud droplet number rival the first indirect effect? *Geophysical Research Letters*, *29*(17). https://doi.org/10.1029/2002gl015295

Su, H., Rose, D., Cheng, Y. F., Gunthe, S. S., Massling, A., Stock, M., et al. (2010). Hygroscopicity distribution concept for measurement data analysis and modeling of aerosol particle mixing state with regard to hygroscopic growth and CCN activation. *Atmospheric Chemistry and Physics*, *10*(15), 7489–7503. https://doi.org/10.5194/acp-10-7489-2010

Wang, B., & Fan, Z. (1999). Choice of South Asian summer monsoon indices. *Bulletin of the American Meteorological Society*, *80*(4), 629–638. https://doi.org/10.1175/1520-0477(1999)080<0629:cosasm>2.0.co;2

Wang, B., Wu, R., & Lau, K.-M. (2001). Interannual variability of the Asian summer monsoon: Contrasts between the Indian and the western North Pacific–East Asian monsoons. *Journal of Climate*, *14*(20), 4073–4090. https://doi.org/10.1175/1520-0442(2001)014<4073:IVOTAS>2.0.CO;2